NATIONAL ADVISORY COMMITTEE
FOR AERONAUTICS

TECHNICAL NOTE 3908

HYDRODYNAMIC CHARACTERISTICS OVER A RANGE OF

SPEEDS UP TO 80 FEET PER SECOND OF A RECTANGULAR MODIFIED

FLAT PLATE HAVING AN ASPECT RATIO OF 0.25 AND OPERATING

AT SEVERAL DEPTHS OF SUBMERSION

By Victor L. Vaughan, Jr., and John A. Ramsen

Langley Aeronautical Laboratory
Langley Field, Va.

Washington

April 1957

NATIONAL ADVISORY COMMITTEE FOR AERONAUTICS

TECHNICAL NOTE 3908

HYDRODYNAMIC CHARACTERISTICS OVER A RANGE OF

SPEEDS UP TO 80 FEET PER SECOND OF A RECTANGULAR MODIFIED

FLAT PLATE HAVING AN ASPECT RATIO OF 0.25 AND OPERATING

AT SEVERAL DEPTHS OF SUBMERSION

By Victor L. Vaughan, Jr., and John A. Ramsen

SUMMARY

An investigation has been conducted to determine the hydrodynamic characteristics over an extended range of speeds (up to 80 feet per second) of a rectangular modified flat plate having an aspect ratio of 0.25 mounted on a single strut and operating at several depths of submersion. Comparisons have been made between these data and data previously obtained over a lower speed range on a similar flat plate having an aspect ratio of 0.25 and having the same plan-form shape and area but one-half the thickness. These comparisons indicated that, in the absence of cavitation, no significant changes existed at the higher speeds investigated. The trends shown in the previous low-speed tests continued to apply.

At high speeds and high angles of attack for depths of submersion of a quarter-chord or more, cavitation at the leading edge grew strong enough to cause a greater decrease in lift coefficient with increasing speed than would be indicated by the results of the previous investigations and the present investigation at the lower angles of attack.

Over the lower speed range covered by the previous investigations and at a given angle of attack, the lift coefficient was slightly lower for the thick model used in the present investigation than for the thin model previously tested.

INTRODUCTION

The results of hydrodynamic investigations of three rectangular flat plates having aspect ratios of 1.00, 0.25, and 0.125 and operating near a free water surface are reported in reference 1. The tares and interferences between the strut used in these investigations and the aspect-ratio-0.25 flat plate are reported in reference 2. Because the

load capacity of the balance used in these investigations was rather limited, it was the factor which determined the speed range. As a result, the range of speeds investigated for the higher angles of attack was reduced to well below the maximum speed of the Langley tank no. 2 towing carriage. The present investigation was undertaken in order to extend the range of speeds to the highest possible towing-carriage speed at which force and moment measurements could be taken for the range of angles of attack up to 20° and in order to investigate more fully the effects of cavitation.

The model used had the same plan-form shape and area as the aspect-ratio-0.25 flat plate reported in references 1 and 2. However, in order for the model to withstand the higher forces caused by the high speeds at high angles of attack, the thickness of the model was doubled and the chord of the supporting strut was increased. This paper presents data obtained in Langley tank no. 2 with the model operating at several depths of submersion. The effects of cavitation are discussed in some detail, and a brief discussion of the effects of vortex ventilation is included.

APPARATUS AND PROCEDURE

Description of Model

The model tested was a rectangular modified flat plate having an aspect ratio of 0.25 and was mounted on a single strut. It had the same plan-form area as the thin aspect-ratio-0.25 flat plate used in the tests of references 1 and 2, but the thickness was doubled in order for the model to withstand the greater loads expected. Both the thin model and the present model had the leading edge rounded to a 2:1 ellipse and the trailing edge symmetrically beveled to provide an included angle of 10°. The increased thickness of the model resulted in a larger leading-edge radius and a longer trailing-edge taper. A drawing of the model is shown in figure 1.

The strut used in this investigation (also shown in fig. 1) had an NACA 66_1-012 airfoil section and was the same as the strut of references 1 and 2 except that the strut chord was increased from 2.6 inches to 4 inches to withstand the larger forces foreseen. The strut was mounted in the same position relative to the model as that used in the previous investigations. For the present investigation this mounting resulted in the station 1.82 inches (0.455 of the strut chord) aft of the strut leading edge being a distance of 45 percent of the model length forward of the model trailing edge. The strut was mounted perpendicular to the model, and there were no fillets at the intersection. Both the model and the strut were made of stainless steel and polished to a smooth finish.

Test Methods and Equipment

Tests were made by using the Langley tank no. 2 towing carriage with electrical strain-gage balances to measure independently the lift, drag, and pitching moment. The pitching moment was measured about an arbitrary point above the model, and the data obtained were used to calculate the pitching moment about the trailing edge of the model.

For all tests a wind screen was used to reduce the aerodynamic tares and aerodynamic effects on the flow patterns to negligible values. Force measurements were made at constant speeds for fixed angles of attack and depths of submersion. Depth of submersion is defined as the distance from the undisturbed water surface to that part of the model closest to the water surface. Tests were made at depths of submersion of 0.5, 1.0, 3.0, and 6.0 inches over a range of angles of attack from 2° to 20° and at speeds up to 80 feet per second.

The changes in angle of attack and the accompanying changes in depth of submersion due to the structural deflections were measured during the calibration of the balances and proved to be negligible for the combinations of forces encountered. The estimated accuracy of the measurements is as follows:

Angle of attack, deg . . . . ±0.1
Depth of submersion, in. . . . . ±0.05
Speed, fps . . . . ±0.2
Lift, lb . . . . ±2.5
Drag, lb . . . . ±1.0
Pitching moment, ft-lb . . . . ±0.3

The forces and moments were converted to the usual aerodynamic coefficient form by using a measured value of the density of water of 1.942 slugs/cu ft. The kinematic viscosity measured during the tests was 1.24×10^{-5} ft^2/sec.

RESULTS AND DISCUSSION

Force Data

The data obtained are presented in figures 2 to 4 as plots of lift coefficient, drag coefficient, and pitching-moment coefficient about the trailing edge as a function of speed with angle of attack as the parameter. Data are given for each of the four depths of submersion investigated. The solid lines in these plots are faired lines obtained by fairing and cross-fairing the force and moment data to get a family of curves.

Effect of Cavitation

The speed at which cavitation at the leading edge was visually observed is shown by the vertical arrows in figures 2 to 7. It may be noted that, for a given angle of attack, cavitation occurred at approximately the same speed regardless of the depth of submersion. The speed at which cavitation occurred decreased as the angle of attack increased up to 12° and remained at a constant value of 30 feet per second for higher angles of attack. Vertical arrows for an angle of attack of 16° at a depth of submersion of 0.5 inch and for an angle of attack of 20° at a depth of submersion of 1.0 inch are not included because at these angles and depths the flow around the model was so disturbed that the start of cavitation could not be observed. Flow separation took place before the inception of cavitation for the angle of attack of 20° at a depth of submersion of 0.5 inch. The vertical arrows in figure 5 show the angles at which cavitation was observed at speeds of 30 and 40 feet per second. Cavitation did not occur at a speed of 20 feet per second for the range of angles of attack tested. At speeds of 50 feet per second and greater, cavitation was present at all angles of attack investigated.

The results of the investigations of reference 1 had shown a decrease in lift coefficient and an increase in drag coefficient with the occurrence of cavitation. These results were corroborated in the present investigation for the same speed and angle-of-attack range. However, for the high speeds and high angles of attack at depths of submersion of a quarter-chord or more, the decrease in lift coefficient with increasing cavitation proved to be much greater than would be expected from the results of the previous investigations and the present investigation at the lower angles of attack. The effect may be seen in the lift-data plots of figure 2 and in the plot of lift coefficient against angle of attack presented as figure 5. In figure 5 it is clear that lift coefficient does not vary with speed for angles of attack below 12° and speeds below 50 feet per second. Above these limiting values, a progressive decrease in lift coefficient with increasing speed may be noted.

The decrease in lift coefficient evidently caused a drop in induced drag coefficient that was great enough to decrease the total drag coefficient as shown in figure 3. This decrease reversed the trend observed for the lower speed, lower angle-of-attack conditions with cavitation present. However, for a constant lift coefficient, the drag coefficient increased with increasing speed or increasing extent of cavitation, as shown in figure 6.

The data plots of the pitching-moment coefficient about the trailing edge (fig. 4) show that the effect of cavitation with increasing speed was appreciable only at the high-angle-of-attack, high-speed conditions where a decrease in pitching moment occurred. Otherwise, only a slight change was noted with increasing extent of cavitation.

The effect of cavitation on the lift-drag ratios may be seen in figure 7. Because the drag coefficient increased for a given lift coefficient with the onset of cavitation, it is obvious that the lift-drag ratio is lowered by the presence of cavitation. This fact may be observed in figure 7 where the curves reach a maximum value before cavitation and, in general, show a downward trend with increasing cavitation. Cross plots of the data show that the angle of attack which gives the best lift-drag ratio seems to be somewhere between 8° and 10°. The value of the lift-drag ratio for an angle of attack of 8°, which is the maximum value shown in figure 7, decreased slightly with increasing depth of submersion. Since the strut drag increases directly and linearly, with depth of submersion, this effect was expected.

Effects of Ventilation

Ventilation occurred at high angles of attack and shallow depths of submersion, as it did in the tests described in reference 1. Air was observed to enter the trailing vortices behind the model and proceed forward until it came in contact with the model, at which time flow separation took place. At the highest angles of attack the flow reattached some distance aft of the leading edge to form a partial bubble, as indicated in figures 2(b), 3(b), and 4(b), which grew with increasing speed until the reattachment reached the trailing edge. At this point the full planing bubble, as described in reference 1, occurred. For somewhat lower angles of attack no reattachment of the separated flow took place, and the full bubble formed immediately at the first separation. Very little change in the force and moment characteristics was noted with the formation of the partial bubble, whereas the full bubble caused sharp breaks in the force and moment characteristics at high speeds. These sharp breaks are indicated in figures 2 to 4 and again in the lift-drag-ratio plots (fig. 7) by the horizontal arrows. A study of the inception of this flow separation is given in reference 3.

Comparison of Present Results With Those for Thin Model

The lift and drag characteristics of the present thick model are compared in figure 8 with those of the thin model of aspect ratio 0.25 used in the tests of reference 1. The results shown are for a depth of submersion of 6.0 inches and for the speed range of reference 1 so as to obtain direct comparisons unaffected by ventilation or cavitation. The nonlinearity of the lift curve found in all low-aspect-ratio results is evident for both models. The lift coefficient at a given angle of attack is lower for the present model than for the thinner model used in the investigation of reference 1, but the general character of the curves is the same. The tests of reference 1 indicated that the value of the lift coefficient for a given angle of attack did not vary with speed; this fact was essentially

true for the present investigation for speeds of more than 20 feet per second when the high-speed, high-angle-of-attack cavitation effects were neglected. In the present investigation, however, the lift coefficients at a speed of 10 feet per second were less than those for the higher speeds, possibly due to Reynolds number effect. The lift-drag polar shows that the two models give curves similar in character but with the drag, in general, slightly higher for the thicker model.

The effect on the lift coefficient of changing the depth of submersion is shown in figure 9. The ratio of the lift coefficient at a given depth of submersion to the lift coefficient at the 6.0-inch depth of submersion is presented as a function of the angle of attack with depth of submersion as a parameter in figure 9(a) and as a function of depth of submersion for angles of attack of 2° and 12° in figure 9(b). It may be noted in figure 9(a) that the maximum value of the lift-coefficient ratio occurred at an angle of attack of approximately 12° for both models whereas the minimum value occurred at an angle of attack of 2° which was the lowest angle of attack investigated. At the angles of attack shown in figure 9(b), the data for the thin model previously tested seem to be more or less asymptotic to the value at the 6.0-inch depth of submersion. For the present thick model at an angle of attack of 2° the data show a more gradual increase in lift coefficient with increasing depth of submersion and would seem to be asymptotic to the value at some depth greater than 6.0 inches. The depth of submersion for which surface effects are negligible would therefore be greater for the present thicker model.

Similar plots showing the effect on the drag coefficient of changing the depth of submersion are presented as figure 10. The effects for drag seem to be much the same as those for lift except that a greater depth of submersion is indicated to be necessary to achieve negligible surface effects for both models.

The ventilation boundaries for the two models at a depth of submersion of 0.5 inch are presented in figure 11. The test points represent the first speed at a given angle of attack for which the planing bubble described in reference 1 was noted. For a given angle of attack, the ventilation boundary moved to higher speeds for the present thick model than for the thin model. As previously noted, two types of bubble formations occurred. The formations involving reattachment of the flow after initial separation corresponds to that found for the model of reference 1 and reported in reference 3. At an angle of attack of 16°, transition from this type of bubble formation to that involving no flow reattachment occurs. The latter type is seen to occur at considerably higher speeds. Additional data showing that this second type of bubble is also present for the thinner model at angles of attack of 12° and below are presented in reference 3. A more complete discussion of the phenomenon involved is also presented in reference 3.

CONCLUSIONS

An experimental investigation has been made to determine the hydrodynamic characteristics over an extended range of speeds (up to 80 feet per second) of a rectangular modified flat plate having an aspect ratio of 0.25 and operating at several depths of submersion. The results of this investigation indicated the following conclusions:

1. In the absence of cavitation no significant changes existed at the higher speeds investigated. Trends shown by previous low-speed tests continued to apply.

2. At high speeds and high angles of attack for depths of submersion of a quarter-chord or more, cavitation at the leading edge grew strong enough to cause a greater decrease in lift coefficient than would be indicated by the results of the previous investigations and the present investigation at the lower angles of attack.

3. Ventilation occurred at higher speeds at a given angle of attack for the thick model than for the thin model previously tested.

4. Over the lower speed range covered by the previous investigations and at a given angle of attack, the lift coefficient was lower for the thick model investigated herein than for the thin model investigated in NACA Report 1246.

Langley Aeronautical Laboratory,
    National Advisory Committee for Aeronautics,
        Langley Field, Va., December 7, 1956.

REFERENCES

1. Wadlin, Kenneth L., Ramsen, John A., and Vaughan, Victor L., Jr.:
   The Hydrodynamic Characteristics of Modified Rectangular Flat Plates
   Having Aspect Ratios of 1.00, 0.25, and 0.125 and Operating Near a
   Free Water Surface. NACA Rep. 1246, 1955. (Supersedes NACA TN's 3079
   by Wadlin, Ramsen, and Vaughan and 3249 by Ramsen and Vaughan.)

2. Ramsen, John A., and Vaughan, Victor L., Jr.: Hydrodynamic Tares and
   Interference Effects for a 12-Percent-Thick Surface-Piercing Strut
   and an Aspect-Ratio-0.25 Lifting Surface. NACA TN 3420, 1955.

3. Ramsen, John A.: An Experimental Hydrodynamic Investigation of the
   Inception of Vortex Ventilation. NACA TN 3903, 1957.
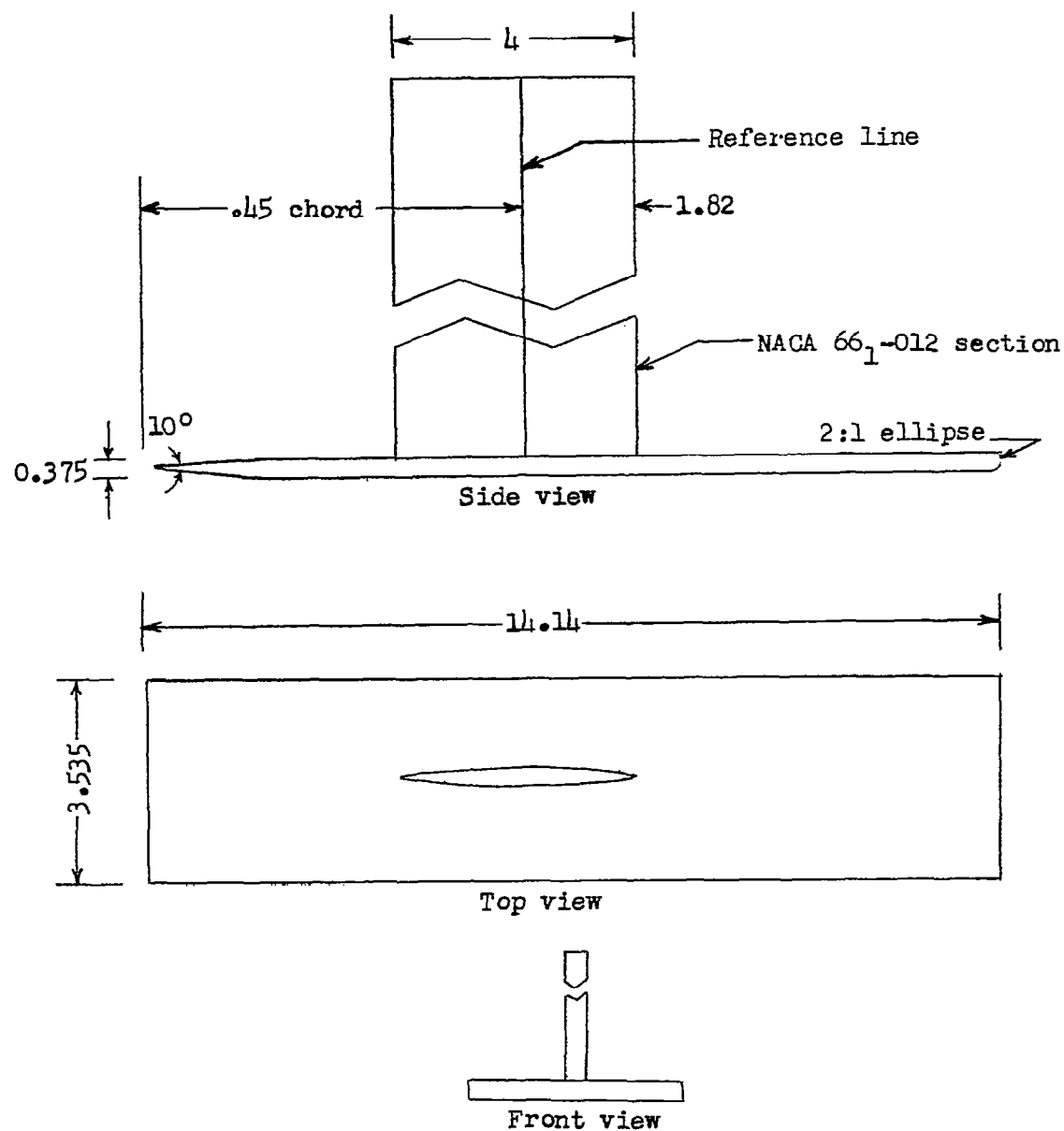
Figure 1.- Details of model.   Dimensions are in inches.
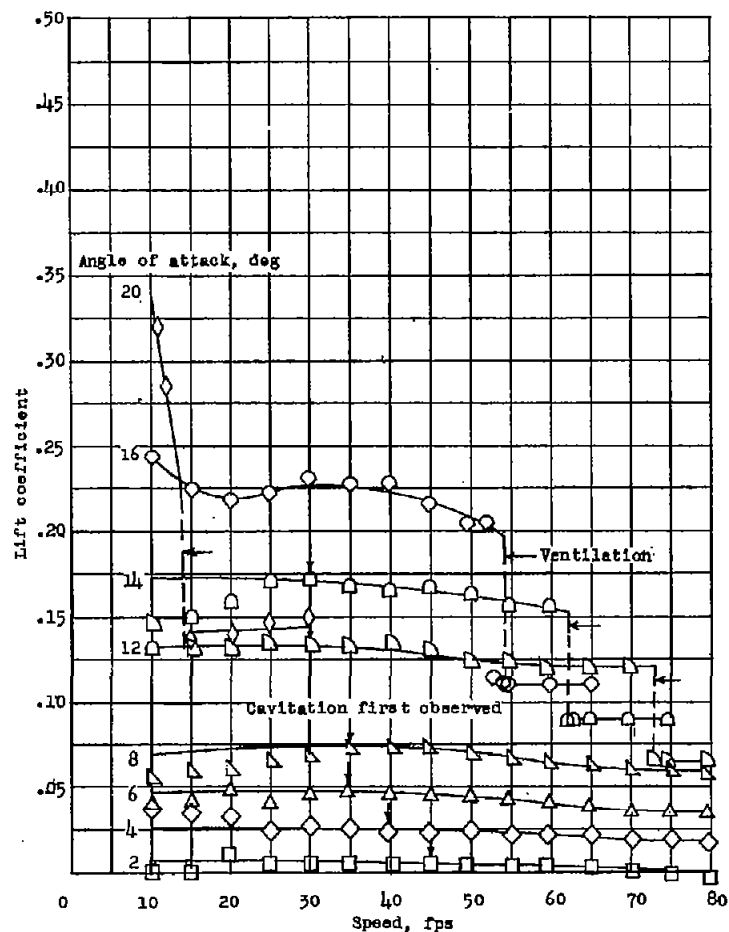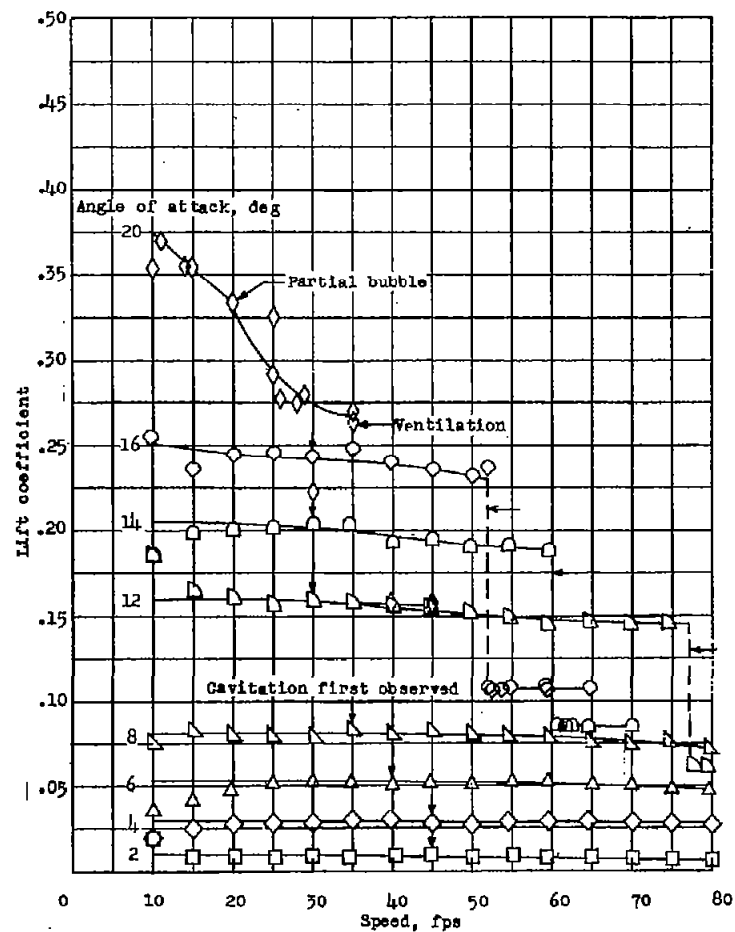
(a) Depth of submersion, 0.5 inch.   (b) Depth of submersion, 1.0 inch.

Figure 2.- Lift characteristics of the aspect-ratio-0.25 flat plate.
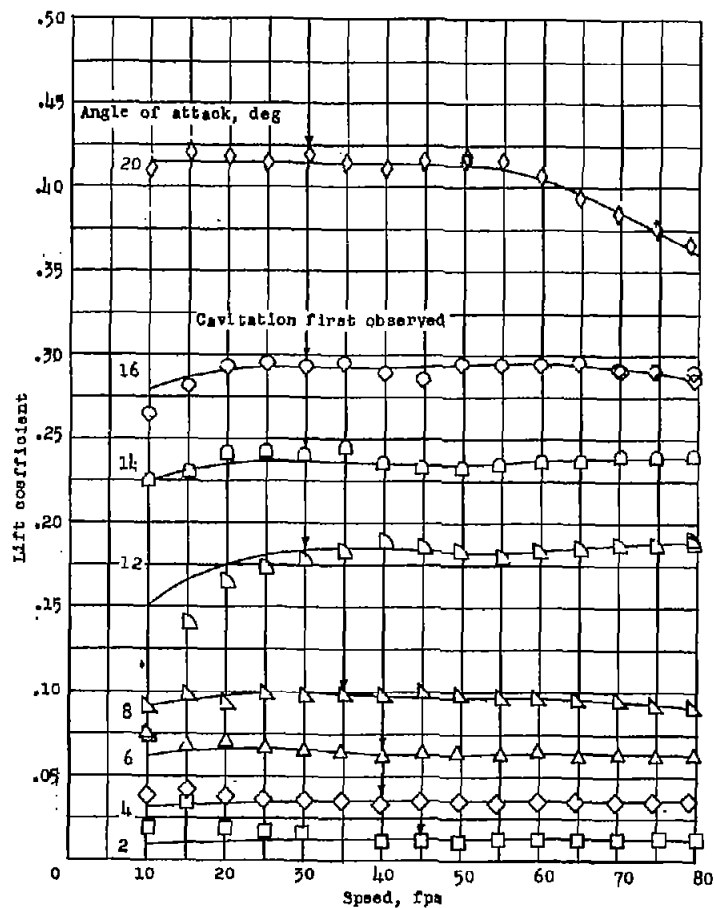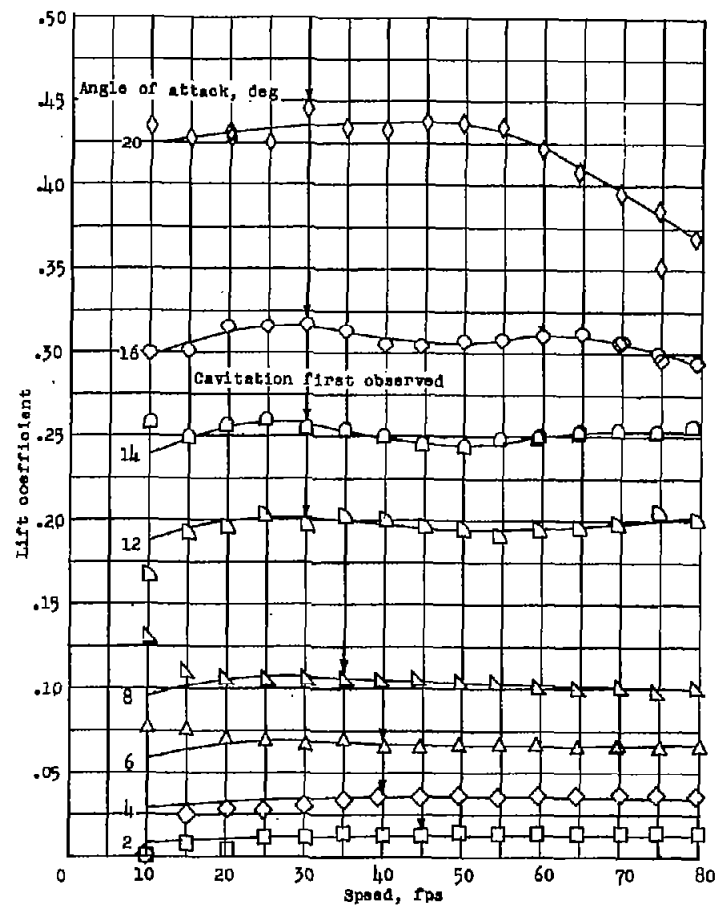
(c) Depth of submersion, 3.0 inches. (d) Depth of submersion, 6.0 inches.

Figure 2.- Concluded.
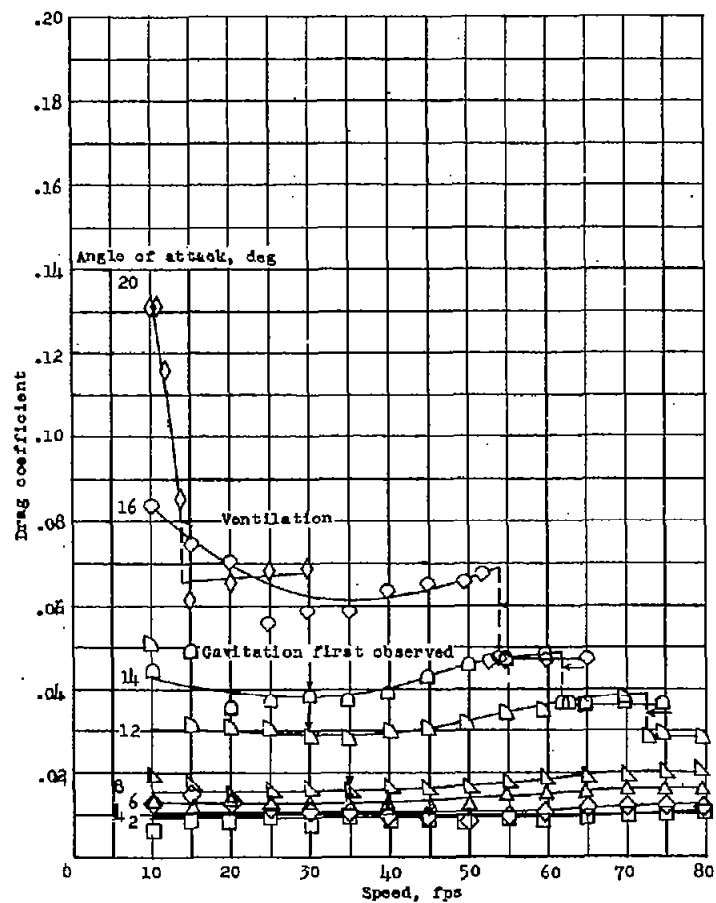
(a) Depth of submersion, 0.5 inch.
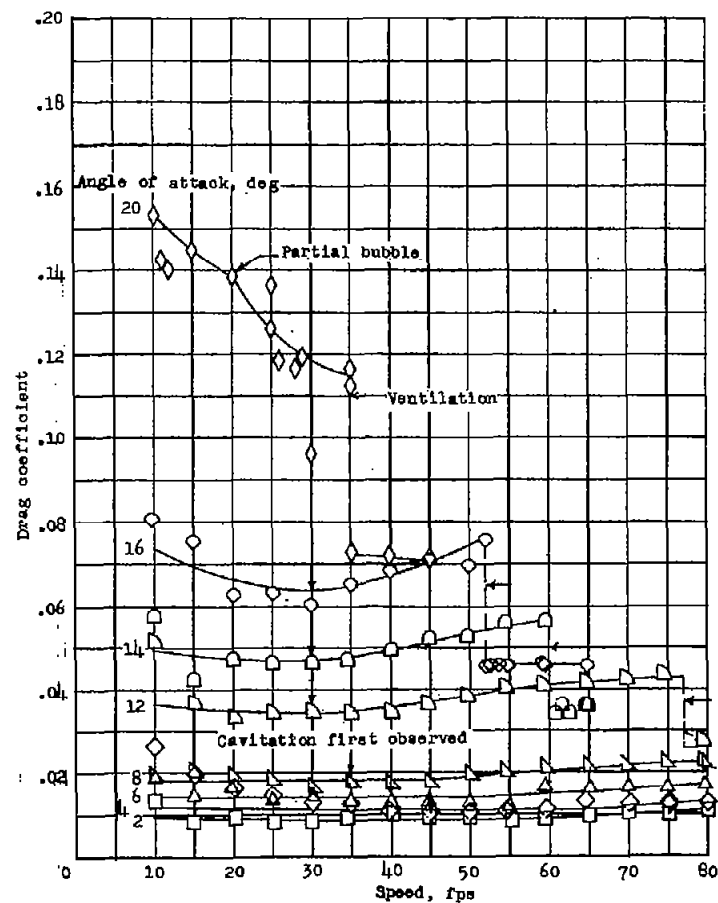
(b) Depth of submersion, 1.0 inch.

Figure 3.- Drag characteristics of the aspect-ratio-0.25 flat plate.
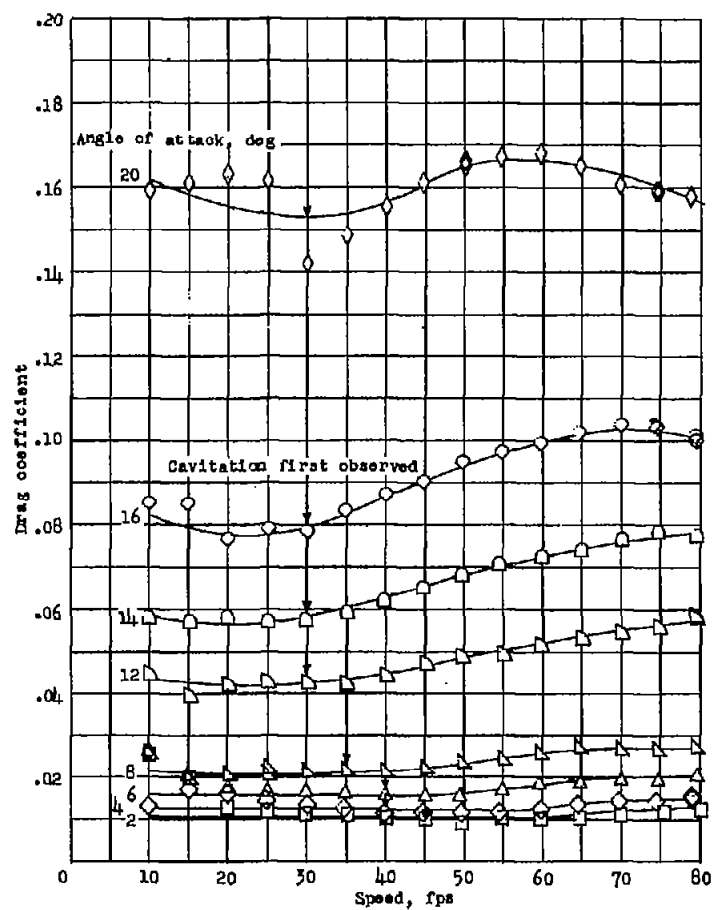
(c) Depth of submersion, 3.0 inches.
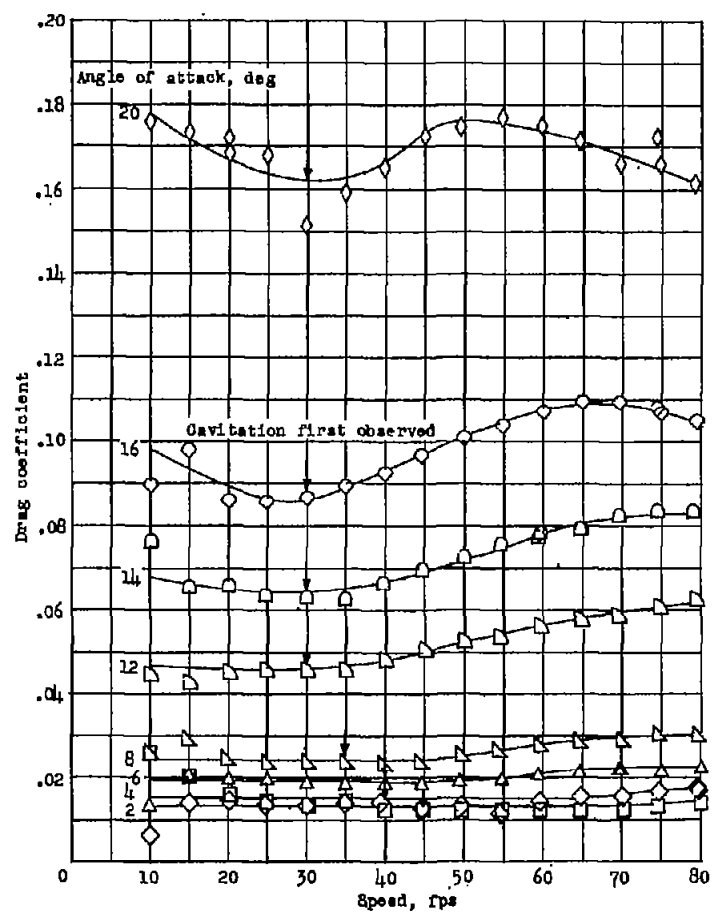
(d) Depth of submersion, 6.0 inches.

Figure 3.- Concluded.
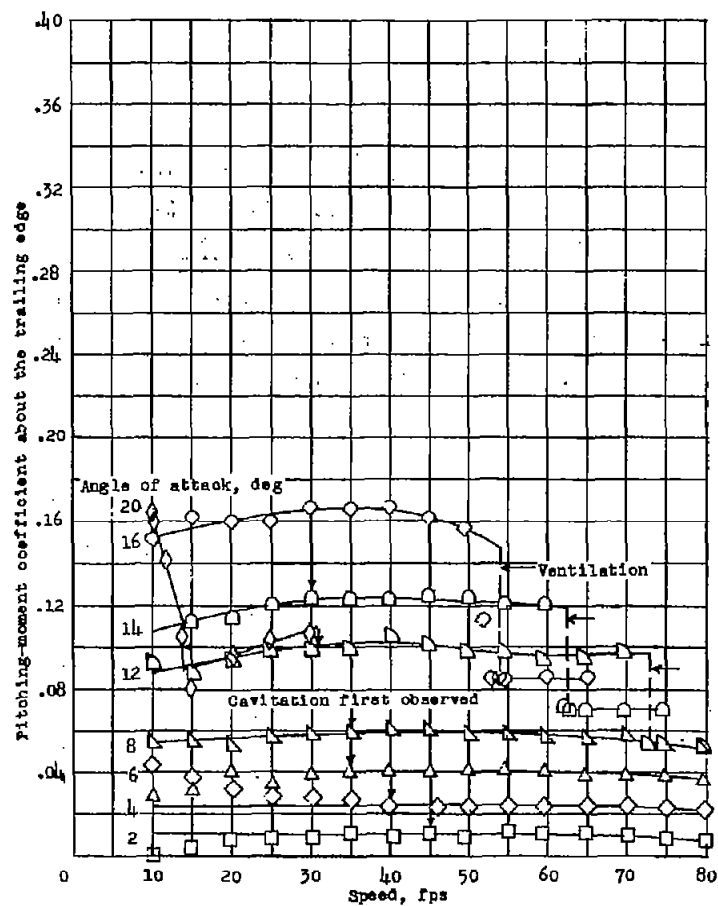
(a) Depth of submersion, 0.5 inch.
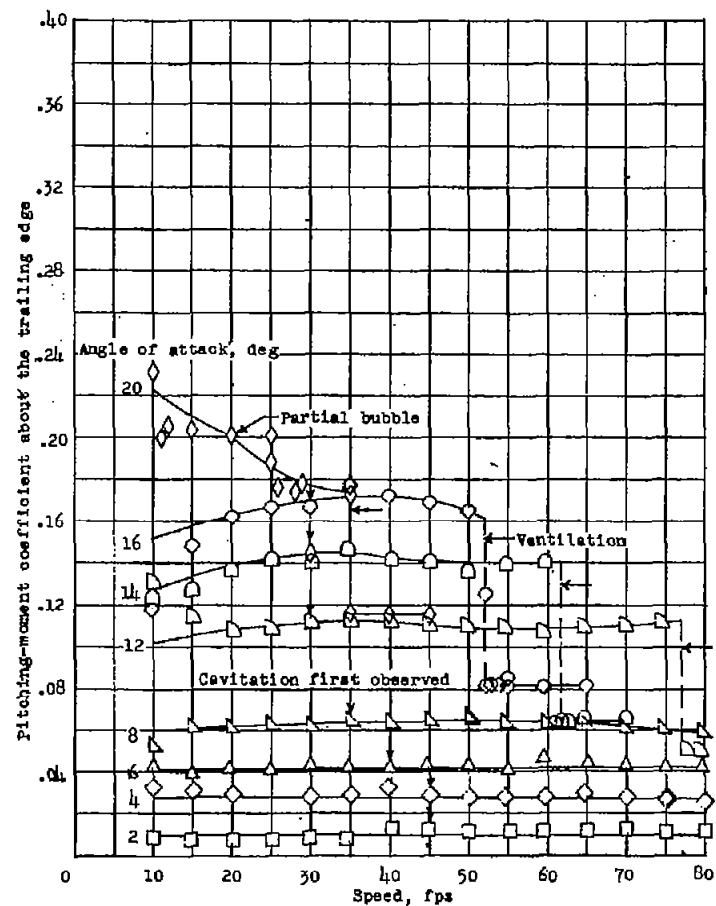
(b) Depth of submersion, 1.0 inch.

Figure 4.- Pitching-moment characteristics of the aspect-ratio-0.25 flat plate.
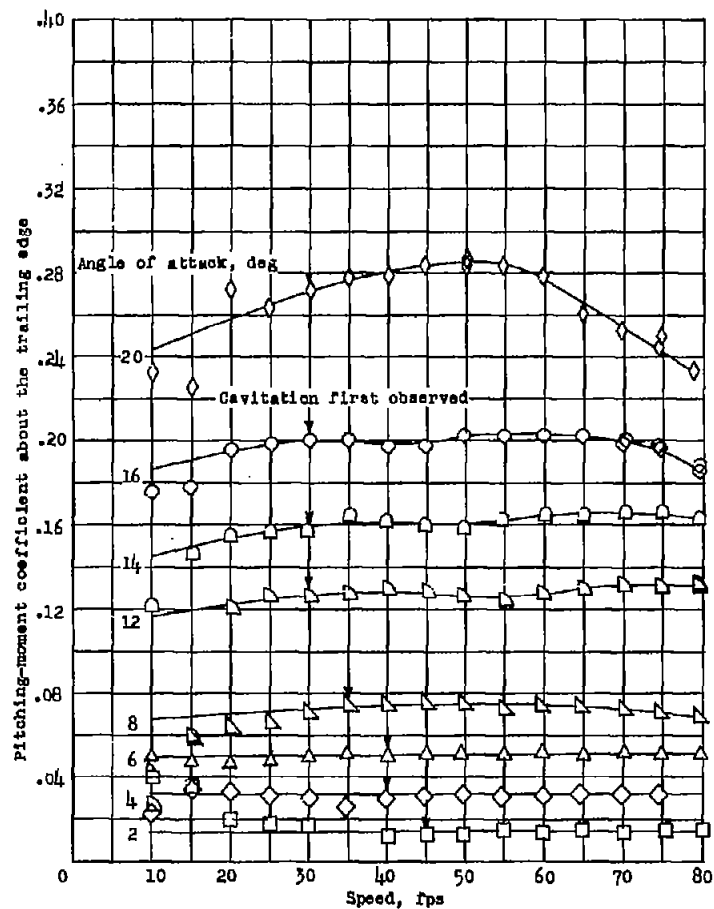
(c) Depth of submersion, 3.0 inches.
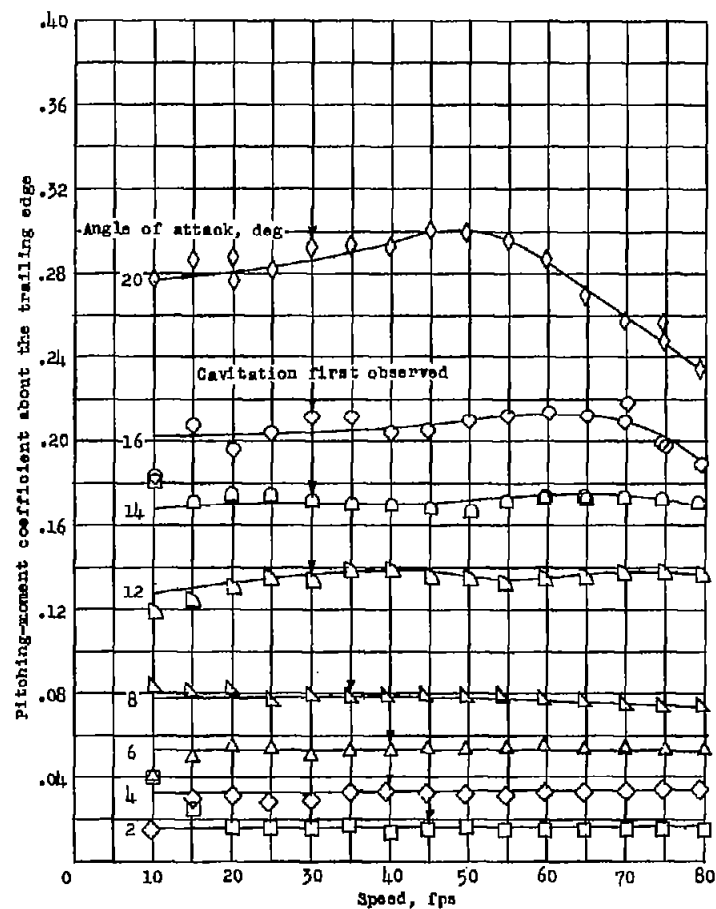
(d) Depth of submersion, 6.0 inches.

Figure 4.- Concluded.
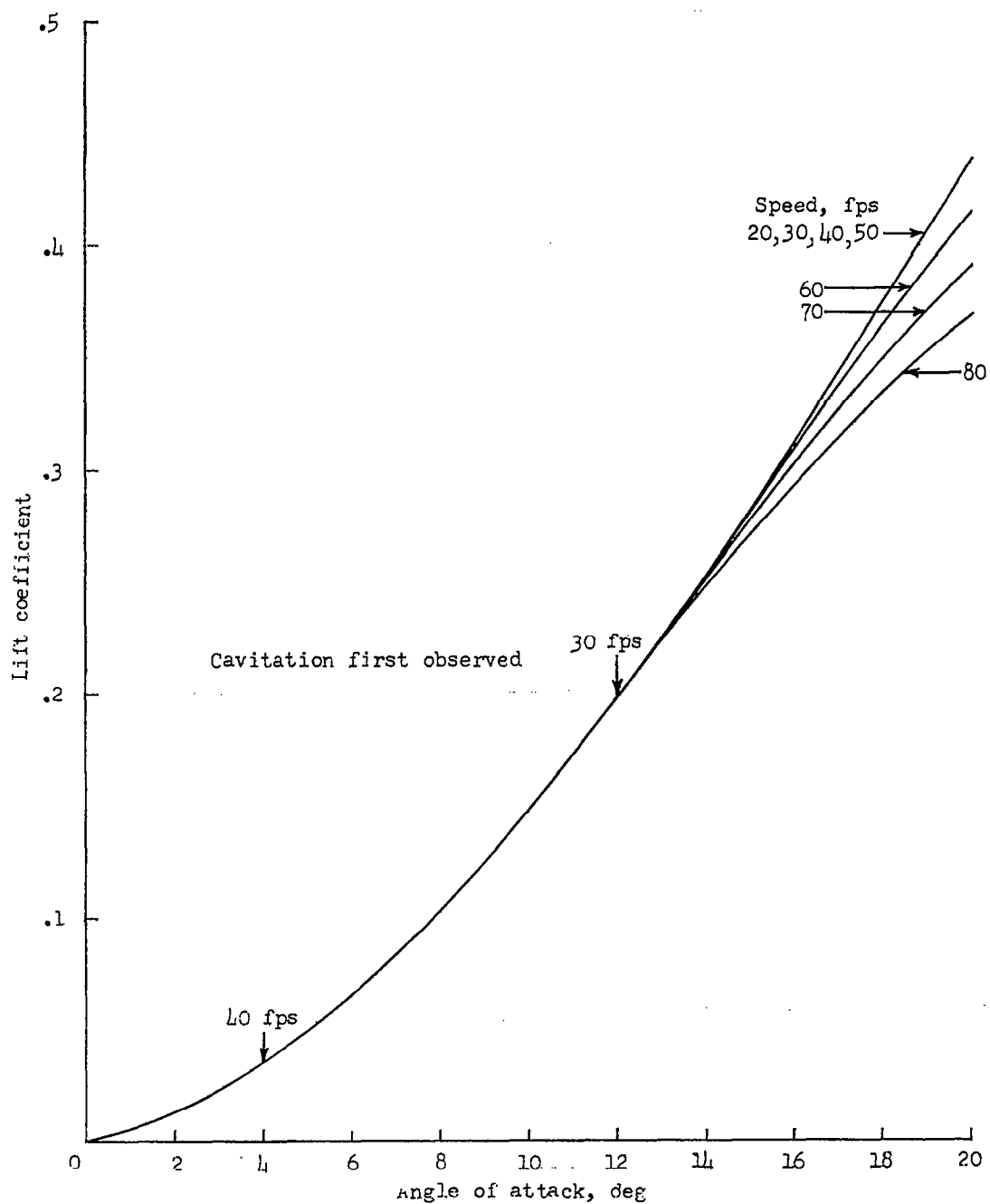
Figure 5.- Effect of cavitation on the lift coefficient at a depth of
    submersion of 6.0 inches. (No cavitation at 20 fps; cavitation present
    at all angles for 50, 60, 70, and 80 fps.)
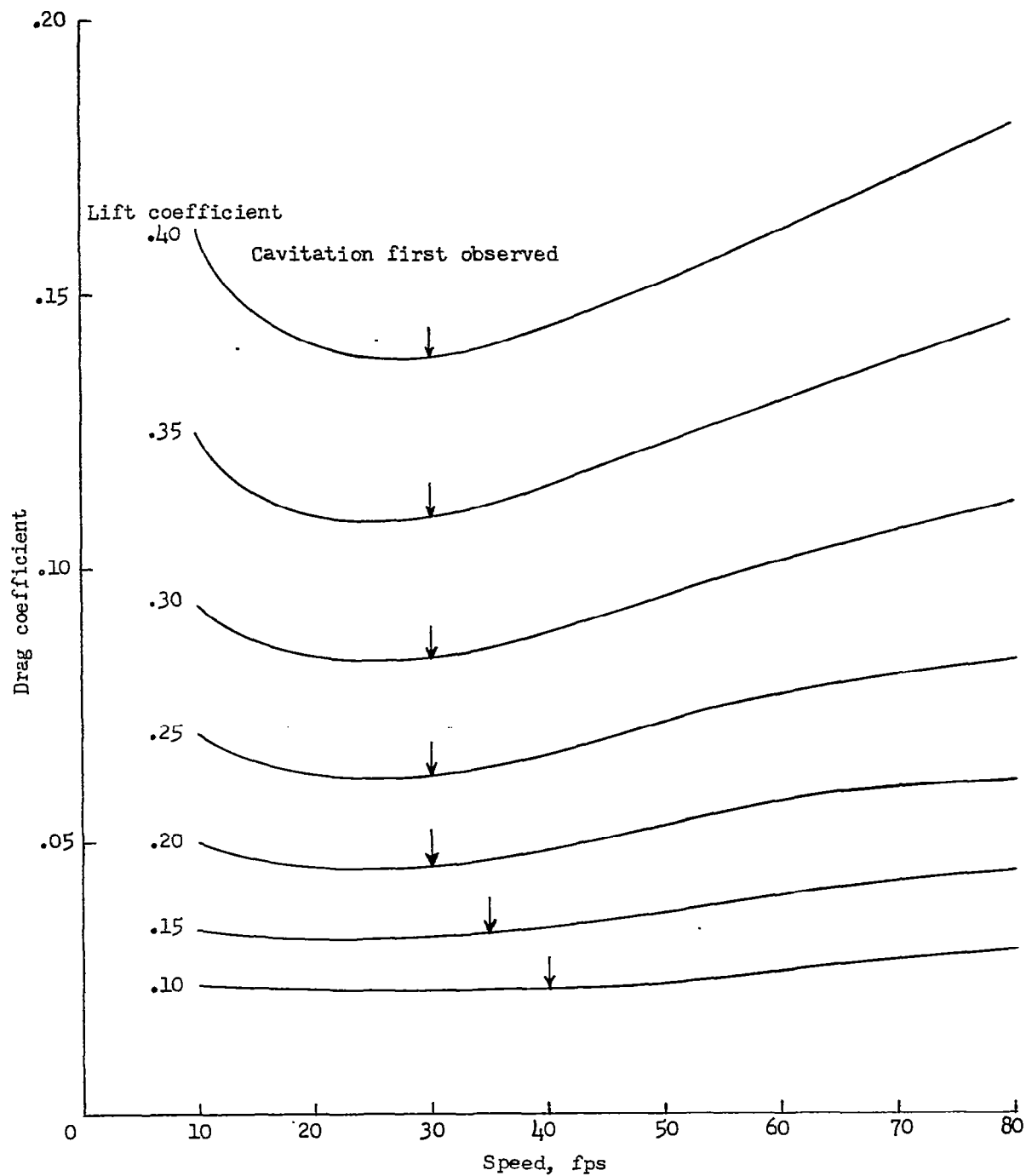
Figure 6.- Effect of cavitation on the drag coefficient at a depth of submersion of 6.0 inches.
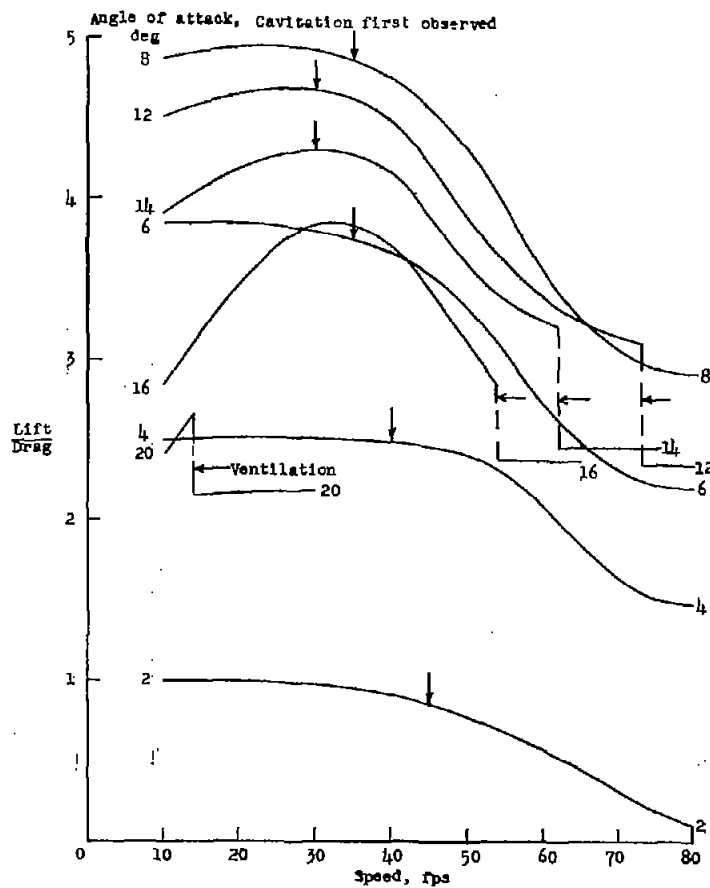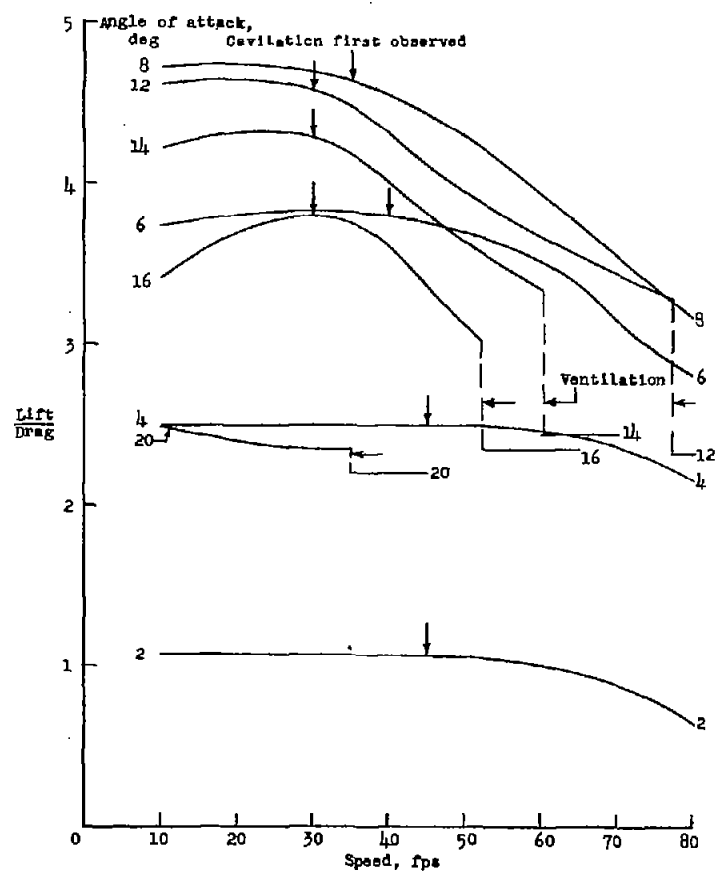
(a) Depth of submersion, 0.5 inch.   (b) Depth of submersion, 1.0 inch.

Figure 7.- Effect of flow changes on the lift-drag ratio.
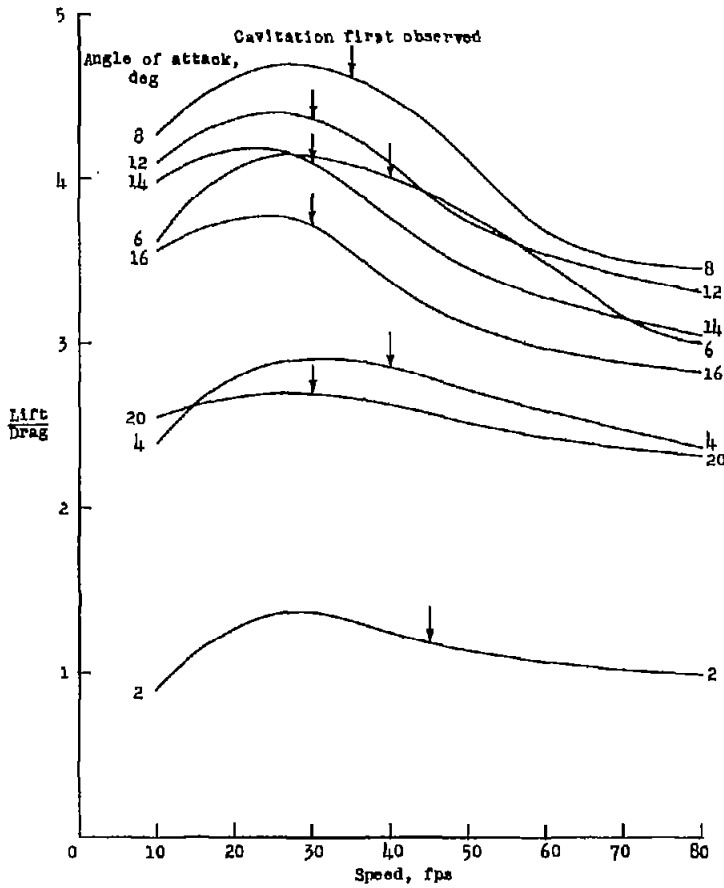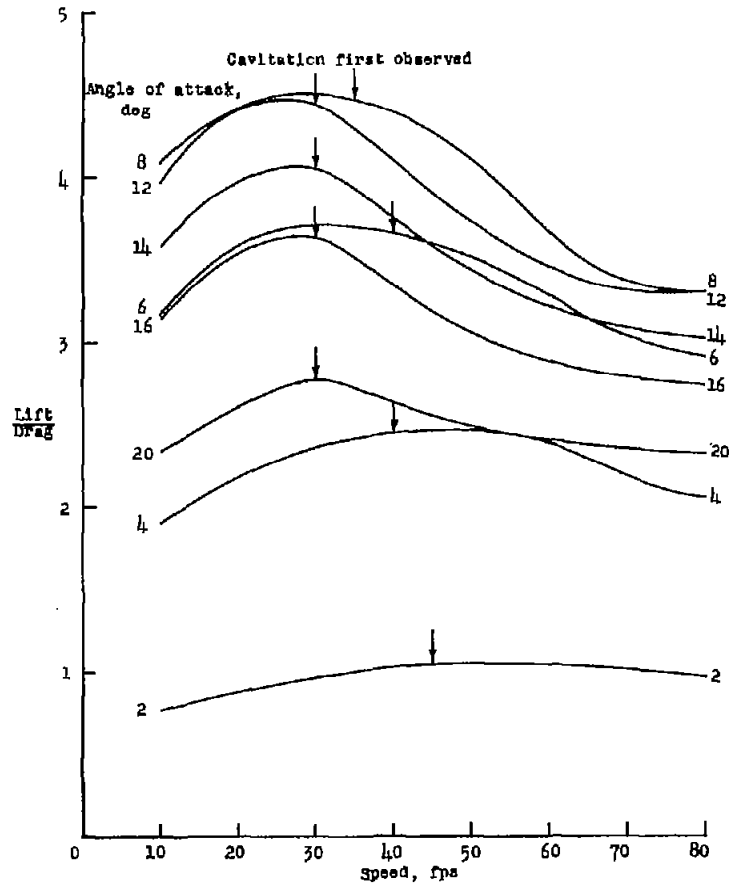
(c) Depth of submersion, 3.0 inches.   (d) Depth of submersion, 6.0 inches.
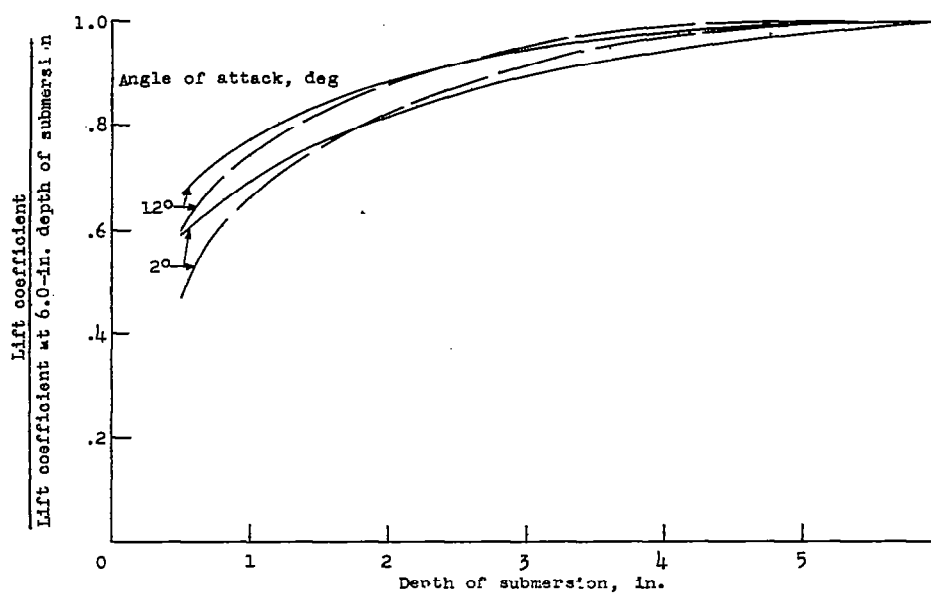
Figure 7.- Concluded.
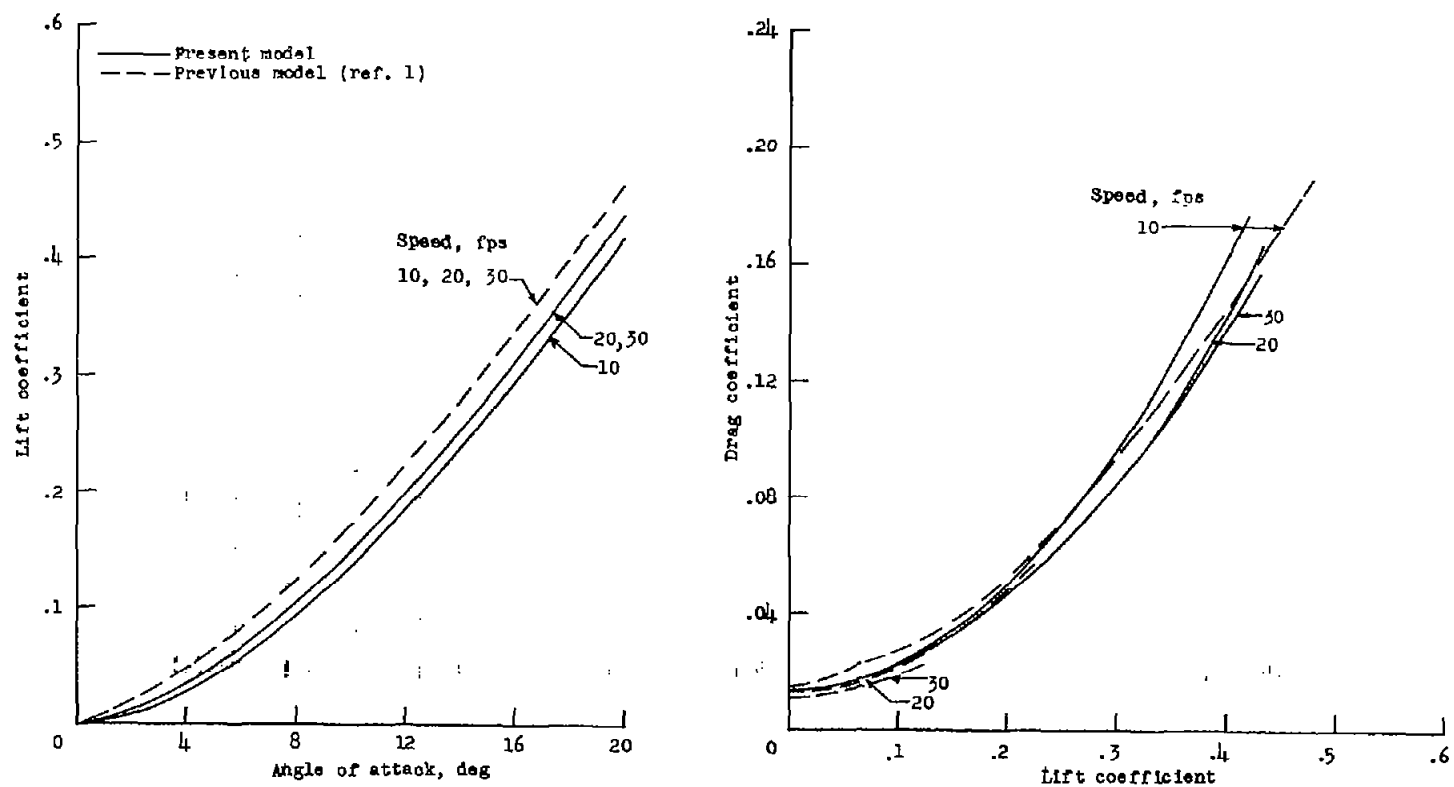
Figure 8.- Comparison of lift and drag characteristics at a depth of submersion of 6.0 inches.
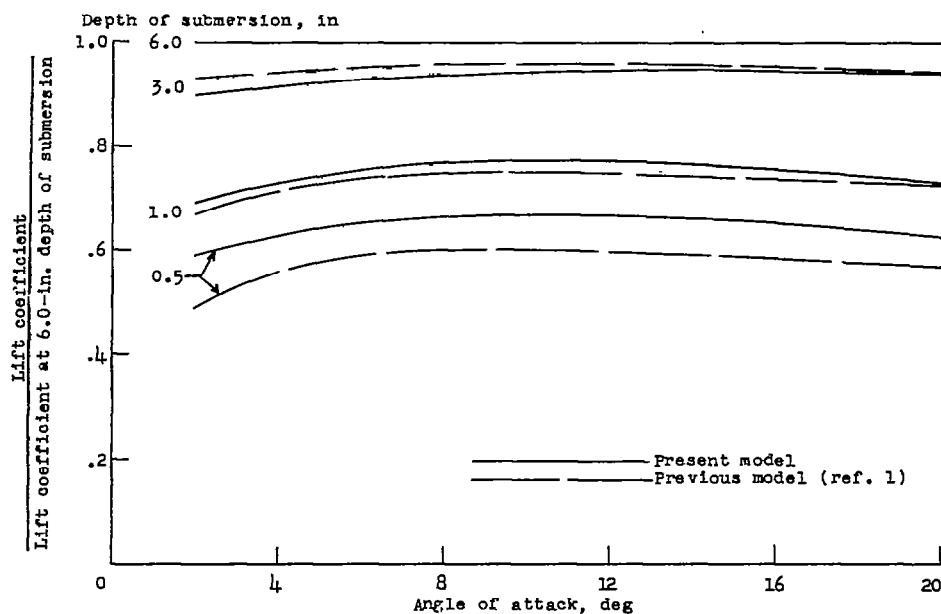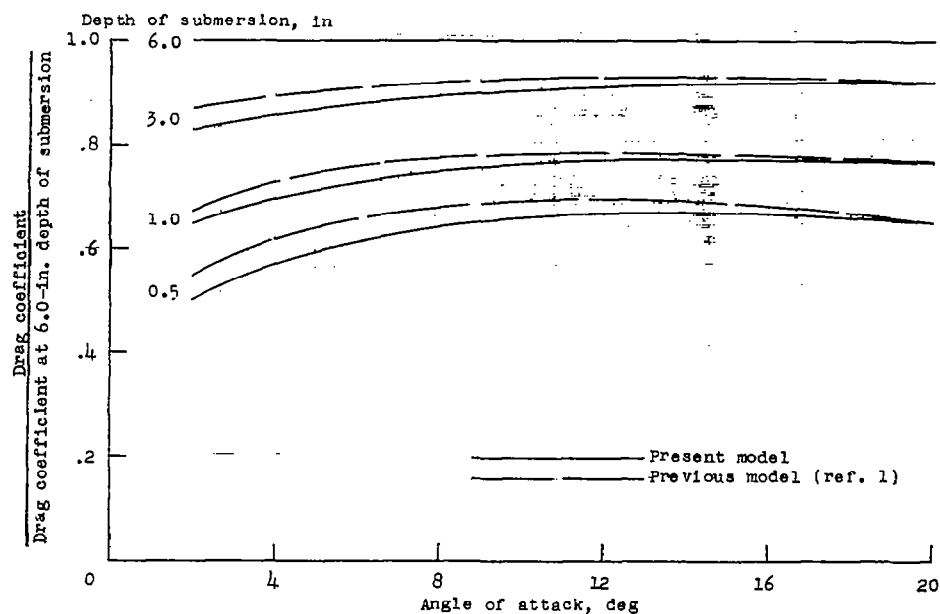
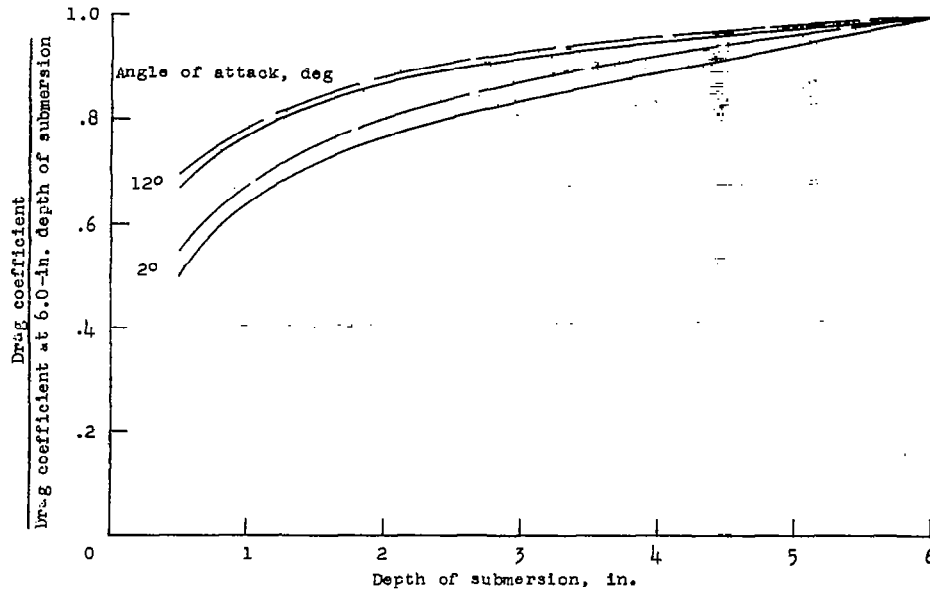(a) Effect of angle of attack.

(b) Effect of depth of submersion.

Figure 9.- Variation of the lift characteristics with angle of attack
and depth of submersion.

(a) Effect of angle of attack.

(b) Effect of depth of submersion.

Figure 10.- Variation of the drag characteristics with angle of attack
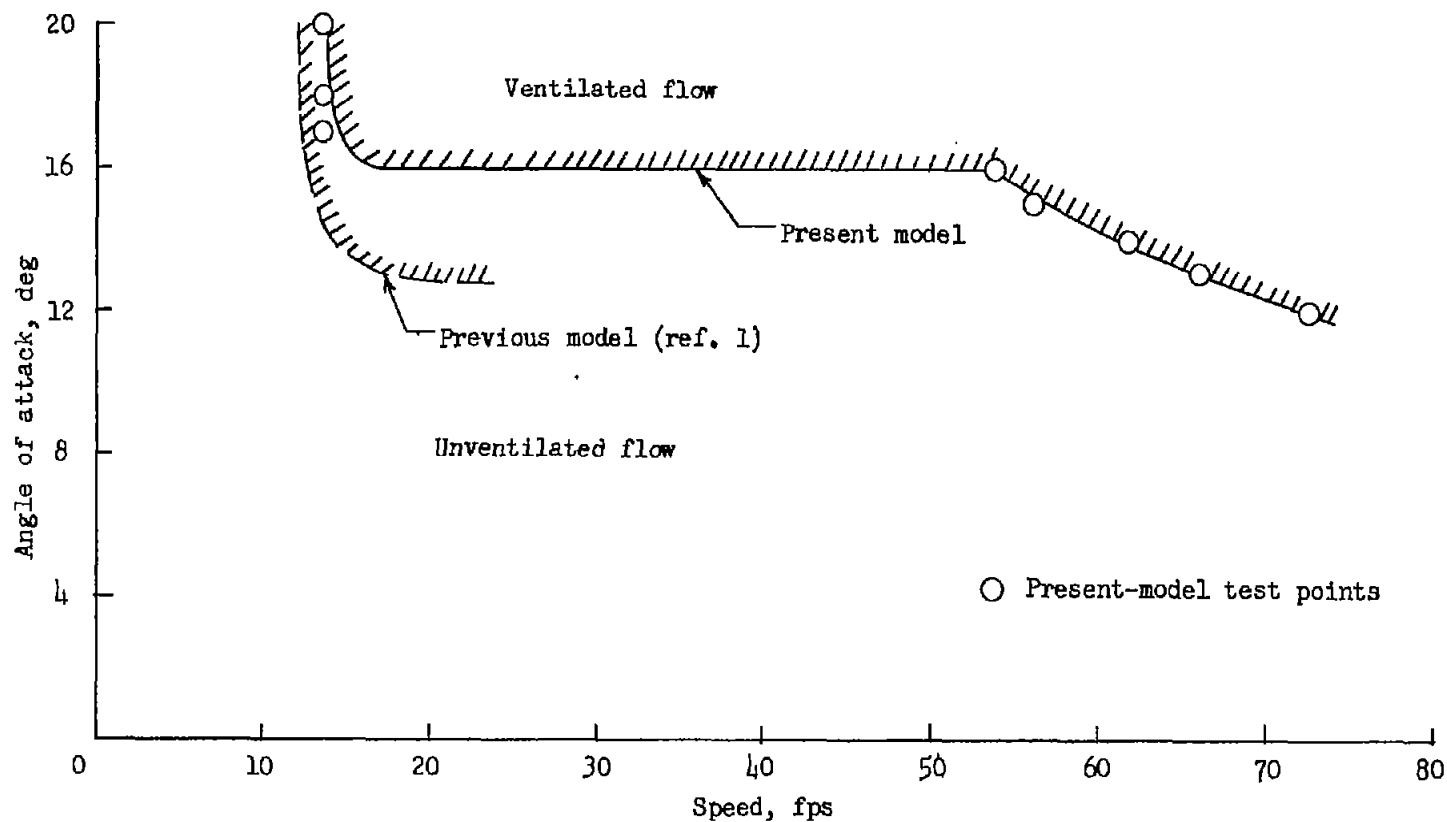and depth of submersion.

Figure 11.- Comparison of ventilation boundaries at a depth of submersion of 0.5 inch.